Proc. 18th Winter Workshop on Nuclear Dynamics (2002) –

18th Winter Workshop on Nuclear Dynamics
Nassau, Bahamas
January 20–27, 2002

Particle Ratios from BRAHMS at $\sqrt{s_{NN}} = 200 GeV$

Peter Christiansen for the BRAHMS collaboration

I. G. Bearden[7], D. Beavis[1], C. Besliu[10], Y. Blyakhman[6], B. Budick[6], H. Bøggild[7], C. Chasman[1], C. H. Christensen[7], J. Cibor[3], R. Debbe[1], E. Enger[12], J. J. Gaardhøje[7], K. Hagel[8], O. Hansen[7], A. Holm[7], A. K. Holme[12], H. Ito[11], E. Jakobsen[7], A. Jipa[10], J. I. Jørdre[9], F. Jundt[2], C. E. Jørgensen[7], R. Karabowicz[4], T. Keutgen[8], E. J. Kim[1], T. Kozik[4], T. M. Larsen[12], J. H. Lee[1], Y. K. Lee[5], G. Løvhøiden[12], Z. Majka[4], A. Makeev[8], B. McBreen[1], M. Mikelsen[12], M. Murray[8], J. Natowitz[8], B. S. Nielsen[7], J. Norris[11], K. Olchanski[1], J. Olness[1], D. Ouerdane[7], R. Płaneta[4], F. Rami[2], C. Ristea[10], D. Röhrich[9], B. H. Samset[12], D. Sandberg[7], S. J. Sanders[11], R. A. Sheetz[1], P. Staszel[7], T. F. Thorsteinsen[9+], T. S. Tveter[12], F. Videbæk[1], R. Wada[8], A. Wieloch[4], and I. S. Zgura[10]

[1] Brookhaven National Laboratory, Upton,New York, [2] Institut de Recherches Subatomiques and Université Louis Pasteur, Strasbourg, France, [3] Institute of Nuclear Physics, Krakow, Poland, [4] Jagiellonian University, Krakow, Poland, [5] Johns Hopkins University, Baltimore, Maryland, [6] New York University, New York, New York, [7] Niels Bohr Institute, University of Copenhagen, Denmark, [8] Texas A&M University, College Station,Texas, [9] University of Bergen, Department of Physics, Bergen,Norway, [10] University of Bucharest,Romania, [11] University of Kansas, Lawrence, Kansas, [12] University of Oslo, Department of Physics, Oslo,Norway, [+]*Deceased*

Abstract. We present preliminary results on charged particle ratios measured in Au+Au reactions at $\sqrt{s_{NN}} = 200$ GeV with the BRAHMS detector at mid and forward rapidities. We find $\pi^-/\pi^+ \approx 1.00 \pm 0.01$ (stat.), $K^-/K^+ \approx 0.95 \pm 0.03$ (stat.), and $\bar{p}/p \approx 0.75 \pm 0.02$ (stat.) at midrapidity ($y \approx 0$). The ratios shows no dependence on transverse momentum or centrality in the range covered. The $\bar{p}/p$ ratio shows a significant dependence on rapidity dropping to 0.27 ± 0.07 (stat.) at $y \approx 3$. The increase in the $\bar{p}/p$ ratio at midrapidity of 17 % from $\sqrt{s_{NN}} = 130$ GeV indicates that a higher degree of transparency has been achieved.

Keywords: heavy-ion collisions, RHIC, particle ratios
PACS: 25.75.-q

ISBN 963 00 0000 0

1. Introduction

Ratios of like charged particles, π^-/π^+, K^-/K^+, and $\bar{p}/p$ are sensitive to the reaction mechanism in Au–Au collisions. In the case of full stopping all the participating baryons will end up in the fireball whereas in the case of full transparency (the Bjorken limit [1]) none of the participating baryons are shifted to midrapidity. A systematic study of stopping at lower beam energies has shown that maximum stopping is reached between $\sqrt{s_{NN}} = 5$ GeV and $\sqrt{s_{NN}} = 17$ GeV [2]. This is supported by new NA49 data at intermediate energies [3]. The first data from RHIC ($\sqrt{s_{NN}} = 130$ GeV) have shown a large increase in the degree of transparency compared to $\sqrt{s_{NN}} = 17$ GeV [4–7].

The BRAHMS experiment at RHIC has collected data at the maximum energy $\sqrt{s_{NN}} = 200$ GeV in 2001 [8]. The data have been analyzed to provide measurements of π^-/π^+, K^-/K^+, and $\bar{p}/p$ ratios, at selected rapidities in the interval $0 \leq y \leq 3$. In the next section the BRAHMS experiment will be described, emphasizing the PID capabilities. Finally results will be shown and their implications will be discussed.

2. The BRAHMS Experiment

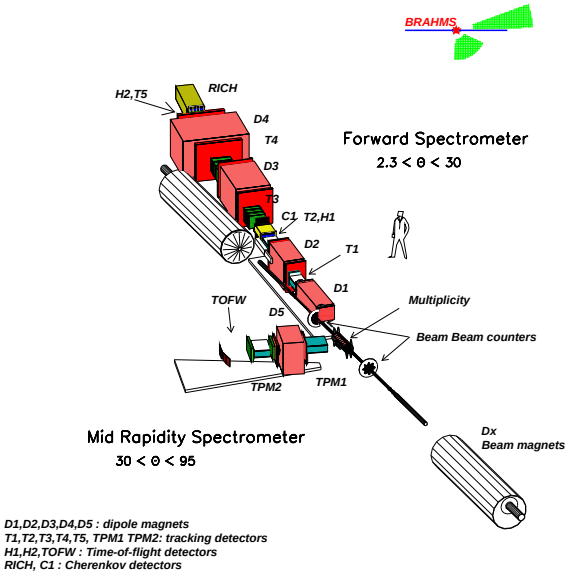

Fig. 1. Birds eye view of the BRAHMS detector. The MRS can be rotated from 90° to 30° and the FS can be rotated between 30° to 2.3°

The BRAHMS experiment, shown in Figure 1, consists of 2 magnetic spectrometers and 3 global detectors [9]. The midrapidity spectrometer (MRS) and the forward spectrometer (FS) can identify π, K, and p, in a small solid angle, 6.5 msr and 0.8 msr respectively. However, by collecting data at many different spectrometer angles a large rapidity interval can be covered, $-0.1 \leq y \leq 3.9$ for pions and $-0.1 \leq y \leq 3.5$ for protons. The polarity and magnitude of the magnetic field in the dipole magnets determines what transverse momentum (p_T) range and charge sign can be measured. The ranges in momentum where particle identification (PID) can be achieved will be discussed below. The 3 global detectors are used for event characterization (such as centrality and interaction point position) and triggering.

2.1. Global Detectors

Like the other RHIC experiments (PHENIX, PHOBOS, and STAR) BRAHMS has two Zero Degree Calorimeters (ZDC) positioned 18 m on either side of the nominal interaction point behind the beam focusing magnets DX. The ZDCs measures the spectator neutrons and can be used as a minimum bias trigger, see [10, 11] for details about the ZDC.

The Beam–Beam counters (BB) are positioned 2.20 m on each side of the nominal interaction point. These detectors consists of two sets of Cherenkov UV–transmitting plastic radiators coupled to photo multiplier tubes (PMTs). Each PMT measures the time signal of the fastest particle and the total energy deposited. The fastest time signal gives the start time ($\sigma_{intrinsic} \approx 60$ ps) for the Time Of Flight (TOF) detectors (see below). By correlating the time information from all tubes the interaction point (IP) can be determined to ≈ 0.6 cm for the high multiplicity data used in this analysis. The energy signal has been used to determine the charged particle multiplicity for very forward particles, $2.1 \leq |\eta| \leq 4.7$, [8, 12].

Close to the nominal interaction point we find the Multiplicity Array (MA) where two different technologies are used to determine the charged particle multiplicity in the pseudorapidity range, $-3.0 \leq \eta \leq 3.0$. The Tile Multiplicity Array (TMA) consists of 35 Plastic scintillator tiles (12 cm $\times$12 cm $\times$0.5 cm) and the Silicon Multiplicity Array (SMA) has 25 Silicon Wafers (4 cm $\times$6 cm $\times$300 μm), each segmented into 7 strips. Both types of detector can be used to measure the charged particle multiplicity [8, 12]. By requiring a minimum of 4 "hits" in the TMA one effectively removes the EM disassociation reactions. Together with the ZDC this trigger includes 95 % of the Au+Au total inelastic cross section. In the offline analysis the event centrality was determined by dividing the integrated MA multiplicity for this trigger.

In most of the data runs a centrality trigger selecting roughly the top 25 % was used to limit the event rate for the Data Acquisition.

2.2. The Midrapidity Spectrometer

The MRS has two Time Projection Chambers (TPCs) for tracking with a dipole magnet in between to allow the determination of the momentum. Matching of the TPC tracks through the magnet is done geometrically using an effective edge approximation of the magnetic

field. Tracks from the front TPC can be projected to the beam line and compared to the IP to reject secondaries and background tracks. The MRS measures charged particles of both charge signs in the same angular and magnetic setting.

The PID of tracks is done using a TOF detector, TOFW, which consists of 125 plastic scintillator slats with PMTs mounted at each end. Combining the TOF and the track length to get the velocity β, one can derive the mass of the charged particle from :

$$m^2 = p^2(\frac{1}{\beta^2} - 1) \tag{1}$$

The effective TOF resolution is $\sigma_{TOFW} \sim 100ps$. This allows separation of π–K to $p \approx 2.0$ GeV/c and K–p separation up to $p \approx 3.5$ GeV/c.

2.3. The Forward Spectrometer

The front part of the FS has the same setup as the MRS except for a magnet in front which sweeps away particles of one charge sign. The TOF detector (H1) has 40 slats with an effective TOF resolution $\sigma_{H1} = 85$ ps. The good TOF resolution and the long path length to H1 (8.6 m) allows the forward going particles ($p > 1$ GeV/c) to be identified. Figure 2 shows the relation between the momentum measured by tracking and the inverse velocity calculated from the TOF. The TOF resolution allows π–K separation up to $p \approx 3.0$ GeV/c and K–p separation can be done up to $p \approx 5.0$ GeV/c.

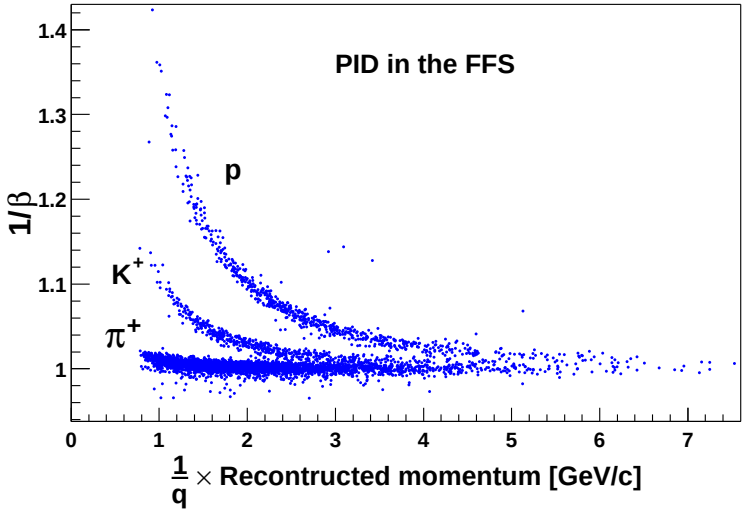

Fig. 2. Particle identification in the FS with H1.

After H1 there is a Cherenkov detector C1. The pion Cherenkov momentum threshold

is 2.6 GeV/c and the kaon threshold is 9.2 GeV/c. This allows us to identify pions up to 9.2 GeV/c and kaons up to 5.0 GeV/c (using H1).

Tracks from the FS can be propagated through the magnet D1 and projected on to a plane transverse to the beam line centered at the IP to remove background and secondaries. The reason for not comparing directly to the IP position along the beam axis is that the resolution of this coordinate determined by a track is proportional with $\frac{1}{\sin\theta}$, diverging at small angles.

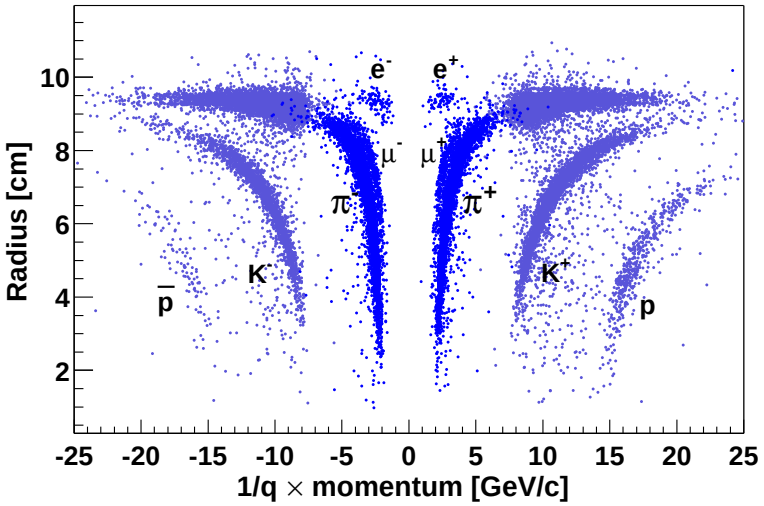

Fig. 3. Particle identification in the FS using RICH. The plot illustrates the RICH performance in 4 settings, low (black) and high (grey) field for both polarities.

In the back of the FS, we have 3 drift chambers (DC) for tracking and another TOF detector, H2, followed by a Ring Imaging Cherenkov (RICH). In the RICH the emitted Cherenkov radiation is focused by a spherical mirror as a ring on the image plane which is read out by 16×20 PMTs. Tracks projected to the image plane can be matched to rings, see Figure 3. From the ring radius and the focal length of the mirror the Cherenkov angle θ_{Ch} can be calculated. The velocity β can then be determined from the relation :

$$\beta = \frac{1}{n \times \cos\theta_{Ch}} \tag{2}$$

where n is the refractive index of the gas. The mass can be derived from equation 1.

3. Results and Discussion

The PID selection is done with a 2σ cut in $1/\beta_{exp} - 1/\beta_{calc}$, where β_{calc} is the velocity calculated from the known mass and the experimentally determined momentum. To measure the ratio of like particles, π^-/π^+, K^-/K^+, and $\bar{p}/p$, data with one charge sign measured at one polarity are compared with data of the opposite charge sign measured at the opposite field polarity, but the same angular setting. Therefore the ratios will be independent of the geometric acceptance for the same IP. The detector inefficiencies cancel out if conditions (background and detector performance) are stable. By calculating the yield of particles per accepted trigger as a function of IP for each polarity setting the ratio can be obtained by dividing the 2 distributions and averaging over the IP distribution afterward. The ratios are not corrected for hyperon decays or antiproton absorption in the beam pipe and spectrometer. At $\sqrt{s_{NN}} = 130$ we found that antiproton absorption increased the $\bar{p}/p$ ratio with 2 % (3.5 %) for the MRS (FS) and that hyperon decays introduced a systematic uncertainty in the same ratio of 5 % [4]. In the MRS, the first p_T bin had a 10 % correction for slow protons originating mainly from pion interactions with the beam pipe. The effect is currently being investigated for the FS (It was negligible at $\sqrt{s_{NN}} = 130$ GeV). Contamination in the PID from misidentification is negligible.

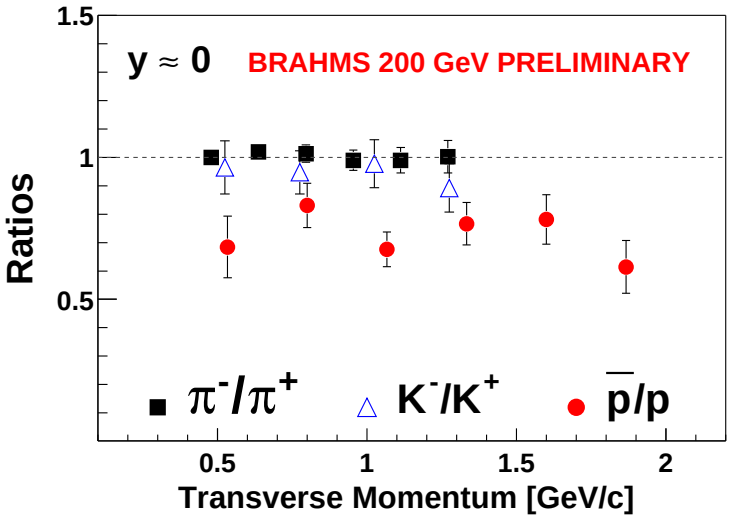

Fig. 4. Ratios of antiparticles to particles vs p_T.

Figure 4 shows the ratios as a function of p_T. They all show little or no dependence on p_T. This indicates that the shape of the p_T–spectrum (the slope) is the same for particle and antiparticle. For a thermal distribution, this means that the temperature is the same. It also means that p_T can be integrated out in the following to get better statistics.

The deviation from unity of some of the particle–antiparticle ratios comes from the original baryons. A simple way to interpret the ratios investigated here are :

$$ratio = \frac{N_{Pair}}{N_{Direct} + N_{Pair}} \tag{3}$$

where N_{pair} is the contribution from pair production and N_{Direct} is the contribution from the beam particles : original protons in the case of the $\bar{p}/p$ ratio and K^+ from associated production ($p + p \rightarrow p + \Lambda + K^+$) in the case of the K^+/K^- ratio.

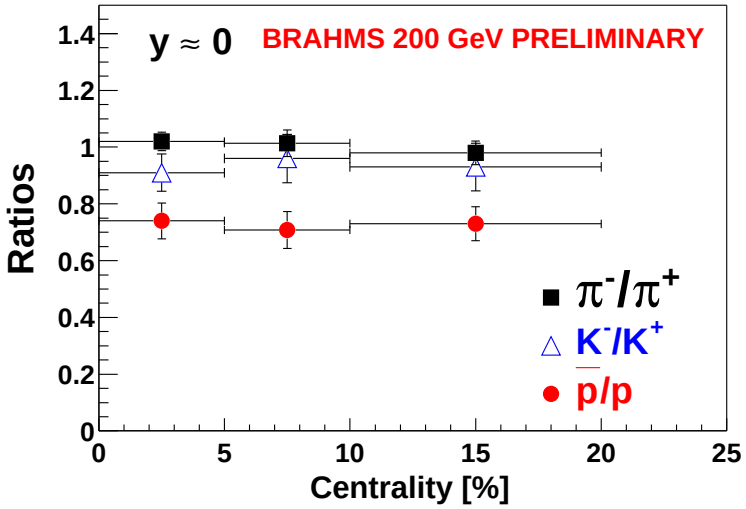

Fig. 5. Ratios vs centrality.

Figure 5 shows that we have no centrality dependence of the ratios in the interval from 20 to 0 %. Over the same interval in centrality we see a 10 % increase in the charged multiplicity per participant [8]. If we assume the same increase in pair production equation 3 would predict that the ratio would increase from 0.75 to 0.77 which this measurement is not sensitive to.

In the following we have integrated over both p_T and centrality to get the ratios at selected rapidities. In Figure 6 the K^-/K^+ and $\bar{p}/p$ ratios at midrapidity, are shown as a function of beam energy $\sqrt{s_{NN}}$. The $\bar{p}/p$ ratio shows the most dramatic increase from 130 GeV [4] to 200 GeV (0.64 to 0.75). In [8] we found that the charged particle multiplicity increased by 14 % at midrapidity from $\sqrt{s_{NN}} = 130$ GeV to $\sqrt{s_{NN}} = 200$ GeV. If we increase the pair production by the same amount and repeat the calculations from the previous paragraph we would predict a rise from 0.64 to 0.67. This is not enough to explain the rise and suggests that fewer baryons are transported to midrapidity.

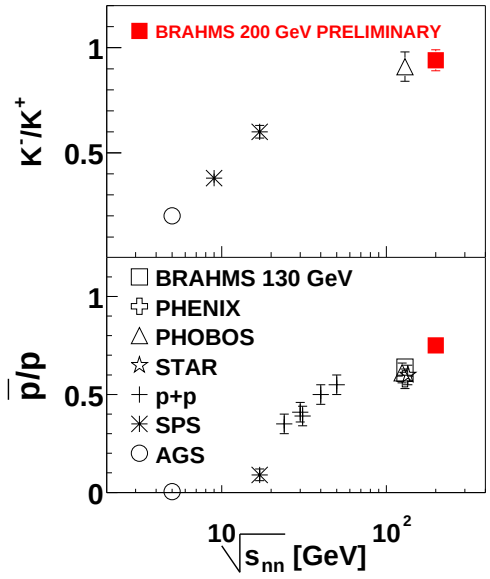

Fig. 6. K^-/K^+ and $\bar{p}/p$ ratios vs beam energy $\sqrt{s_{NN}}$

In thermal models of heavy ion collisions the ratios of all particle species are controlled by the temperature and the chemical potential. In [13], the particle ratios at $\sqrt{s_{NN}} = 200$ GeV/c were predicted using a thermal model assuming the same chemical freeze-out temperature as fitted for $\sqrt{s_{NN}} = 130$ GeV/c, $T \approx 170$ MeV and the empirical formula for the chemical potential $\mu_B \approx 1.3\text{ GeV} \times (1 + \sqrt{s}/4.5\text{ GeV})^{-1}$ ($\mu_B(200\text{ GeV}) \approx 29$ MeV). They find $\frac{K^-}{K^+} \approx 0.93$ and $\bar{p}/p \approx 0.75$. This is in excellent agreement with the measured value of 0.95 ± 0.03 and 0.75 ± 0.02 at midrapidity.

Until now we have only shown ratios at midrapidity, but the same analysis can also be done at forward rapidities. Figure 7 shows the rapidity dependence of the ratios and we notice a strong rapidity dependence of the $\bar{p}/p$ ratio, dropping from 0.75 at midrapidity to 0.27 ± 0.07 (stat.) at $y \sim 3$. This is a big deviation from a boost invariant source where the ratios are constant and indicates that as we go away from the baryon poor central region, we reach a baryon rich fragmentation region. The π^-/π^+ ratio is flat over the full range. The K^-/K^+ ratio is perhaps decreasing a little as we go up in rapidity, but the level is high (> 0.8) over the full range. The behavior of the K^-/K^+ ratio shows that the particles from associated production, in contrast to the original protons, almost has the same distribution as the particles from pair production in the wide rapidity interval covered.

Let us finally address the question about stopping, transparency, and the Bjorken limit. In p-p collisions we observe that the midrapidity region is depleted of net-baryons as beam energy increases [2]. This leads us to believe that the same would happen in heavy ion collisions. When talking about the Bjorken limit one should therefore remember that even

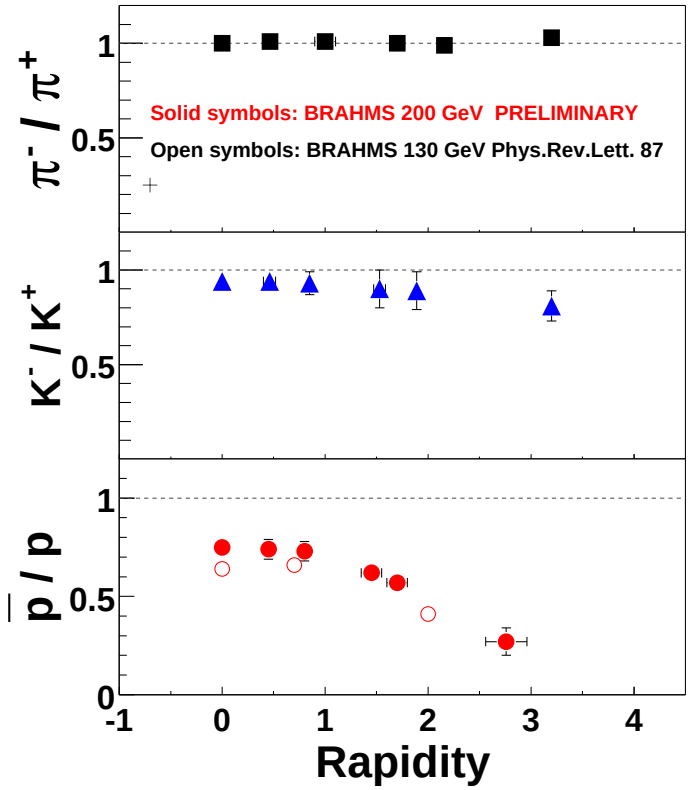

Fig. 7. Ratios as a function of rapidity. The 3 first points are from the MRS, the last 3 are from the FS. The PID for the first 2 FS points was done with H1 and C1 and the last point was done with the RICH.

in p-p collisions the $\bar{p}/p$ ratio is not much closer to unity than found here. CERN ISR data extrapolated to 200 GeV/c gives $\bar{p}/p \approx 0.87 \pm 0.1$ [14], so ideally this is the maximum limit we would expect. There are however differences between the two systems that make the comparison difficult. In heavy-ion collisions the number of binary collisions makes a significant contribution to the charged multiplicity so a nucleon in the Au-Au collision is likely to make several interaction resulting in a higher rapidity loss [2] and an enhanced charged particle production than a proton in a p-p collision. Absorption of antiprotons in the fireball [15] decreases the ratio. In Au-Au collisions we also have p-n and n-n interactions and the $\bar{p}/p$ ratio from these collisions does not have to be the same as from p-p collisions.

4. Conclusions

The BRAHMS experiment has measured ratios of antiparticle/particles. At midrapidity we find $\pi^-/\pi^+ \approx 1.00 \pm 0.01$ (stat.), $K^-/K^+ \approx 0.95 \pm 0.03$ (stat.), and $\bar{p}/p \approx 0.75 \pm 0.02$ (stat.). The ratios show no dependence on centrality and p_T in the covered range at this sensitivity level (≈ 5 %) indicating that the slopes of the spectra are identical for particles and antiparticles. The levels of the ratios are in good agreement with what was predicted with a thermal model [13]. The increase in the antiproton to proton ratio from $\sqrt{s_{NN}} = 130$ GeV to 200 GeV indicates that fewer net protons are present at midrapidity, i.e., a higher degree of transparency has been achieved than at 130 GeV.

The rapidity dependence for the ratios are quite different. The antiproton to proton ratio decreases significantly from 0.75 at midrapidity to 0.27 ± 0.07 (stat.) at $y \sim 3$. The K^-/K^+ ratio is remarkable flat indicating that the transport mechanisms in the reaction are different for protons and K^+. The rapidity dependence also shows that it takes more than just a chemical potential and temperature to describe the data. Finally one could speculate that as we go to the very forward rapidities ($y > 1$), we start seeing the protons that has escaped the formating fireball.

References

1. J.D. Bjorken *Phys. Rev. D.* **27** (1983) 140
2. F. Videbæk and O. Hansen *Phys. Rev. C.* **52** (1995) 2684
3. V. Friese et al., hep-ph/0111423, submitted to *World Scientific*
4. I.G. Bearden et al., *Phys. Rev. Lett.* **87** (2001) 112305
5. B.B. Back et al., *Phys. Rev. Lett.* **87** (2001) 102301
6. C. Adler et al., *Phys. Rev. Lett.* **86** (2001) 4778
7. C. Adler et al., *Phys. Rev. Lett.* **87** (2001) 262302
8. I.G. Bearden et al., nucl-ex/0112001, Accepted for publication, *Phys. Rev. Lett.* (2002)
9. M. Adamczyk et al., http://Cyclotron.tamu.edu/hagel/BrahmsNIMPaper.ps, submitted to *Nucl. Inst. Meth.*
10. M. Chiu et al., nucl-ex/0106016, submitted to *Phys. Rev. Lett.*
11. C. Adler et al., *NIM A* **470** (2001) 488
12. I.G. Bearden et al., *Phys. Lett. B* **523** (2001) 227.
13. P. Braun–Munzinger et al., *Phys. Lett. B* **518** (2001) 41.
14. K. Guettler et al., *Nucl. Phys. B* **116** (1976) 77. Extrapolation done by Hans Bøggild, private communications.
15. M. Gonin and O. Hansen, *Eur. Phys. J. A* **7** (2000) 293.